AIMs: a new strategy to control physical aging and gas transport in mixed-matrix membranes

Journal of Materials Chemistry A

PAPER

View Article Online
View Journal | View Issue

Cite this: J. Mater. Chem. A, 2015, 3, 15241

AIMs: a new strategy to control physical aging and gas transport in mixed-matrix membranes†‡§

Melanie Kitchin,[ab] Jesse Teo,[b] Kristina Konstas,[a] Cher Hon Lau,[ab] Christopher J. Sumby,[b] Aaron W. Thornton,[a] Christian J. Doonan*[ab] and Matthew R. Hill*[ab]

Received 30th March 2015
Accepted 19th June 2015

DOI: 10.1039/c5ta02286j

www.rsc.org/MaterialsA

The effect of controlling interactions between the components in a mixed-matrix membrane at the molecular level has been explored. A systematic series of soluble metal–organic polyhedra (MOPs) of varying external organic chain length were prepared and applied within polymer membranes to produce anti-aging intercalated membranes (AIMs). Use of a soluble porous additive allowed for intimate mixing between the polymer and the porous additive, eliminating the formation of non-selective gas transport voids at the interface, typically found in traditional mixed-matrix membranes. Moreover, the molecular interaction thus created provided a valuable tool for tailoring the physical aging rates of the membranes. Aging was slowed by a factor of three with the optimal ^{t}Bu-MOP additive, and viscosity measurements revealed they held the strongest MOP–polymer interaction, confirming the utility of the AIMs approach. MOP loading was therefore able to be optimized for the maximum anti-aging effect by monitoring the relative change in viscosity. Absolute gas permeability scaled with the MOP external organic chain length, revealing solubility-driven diffusion.

The realization of polymer-based membrane technologies in industrial applications requires sustainable performance of a material over an extended period of time. Unfortunately, the polymeric structures that demonstrate the most attractive initial permeability and selectivity properties are marred by physical aging processes that reduce fractional free volume content and increase chain packing density[1] as large cavities collapse towards an unattainable thermodynamic equilibrium.[2]

Given the potential application of polymeric membranes in low-energy separation processes, there has been a large amount of research aimed at locking as-cast polymers into place to retain initial high fractional free volume content, offsetting physical aging. One approach has been to post-synthetically pyrolyse precursor polymers at high temperatures to rigidify polymer chains and form dense carbon molecular sieves.[3] Another approach has been to use additives such as nanoparticles or microporous fillers, to prop open and increase transport pathways. Such composite materials, known as mixed-matrix membranes ('MMMs') have been prepared using metal–organic frameworks (MOFs), zeolitic imidazolate frameworks (ZIFs) and fused silica as the inorganic additive,[4,5] to mixed success. MOF-based MMMs are based around the adsorption and diffusion behaviour of gas molecules through the embedded MOFs rather than retaining the size-sieving properties of the surrounding polymer. As the polymer chains relax, access to the MOF pores throughout the film is restricted.

Another challenge faced by MOF- and ZIF-based MMMs is that of poor dispersion of, and in many cases interaction between, polymer and additive materials.[6] Poor adhesion at the additive–polymer interface generates voids that compromise membrane selectivity, thereby limiting industrial feasibility (Fig. 1).

Therefore, new additives that give rise to more intimate interactions with the polymer matrix are desirable for improving gas transport[7,8] and the rate of physical aging.[9] Adhesion between the additive and the matrix has previously been achieved using interfacial agents, modified particle surfaces, and ionic liquids.[6,10,11] We recently reported[9] that physical aging could be addressed through a strong interaction of the carbonaceous pores of PAF-1 [12] with polymer side-chains.

Unlike porous aromatic frameworks, MOFs and other related extended nanoporous frameworks, metal organic polyhedra (MOPs) are comprised of individual porous molecular cages.[13] As demonstrated by Balkus *et al.* their discrete molecular nature makes them amenable to solution processing, and as a result they can be homogeneously dispersed within the host

[a]Manufacturing, CSIRO, Bayview Avenue, Clayton, VIC, 3168, Australia. E-mail: Christian.Doonan@adelaide.edu.au; Matthew.Hill@csiro.au

[b]Centre for Advanced Nanomaterials, The School of Chemistry & Physics, The University of Adelaide, Adelaide, SA, 5005, Australia

† MRH acknowledges FT1300345. Parts of this work were funded by the Science and Industry Endowment Fund (SIEF).

‡ The manuscript was written through contributions of all authors. All authors have given approval to the final version of the manuscript.

§ Electronic supplementary information (ESI) available. See DOI: 10.1039/c5ta02286j

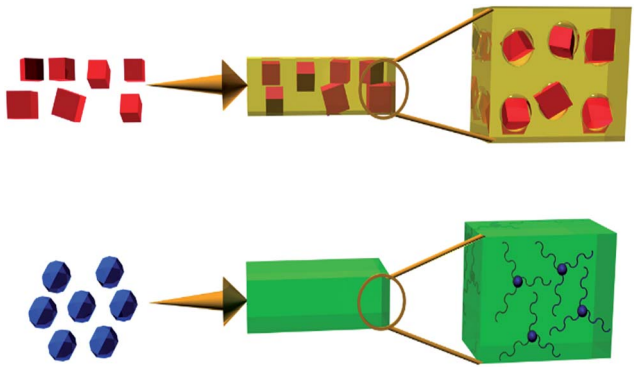

Fig. 1 Use of the soluble metal organic polyhedra (MOPs) in mixed matrix membranes (bottom) allows for intercalation that addresses physical aging, as opposed to the nonselective transport pathways created by insoluble additives such as MOFs (top).

polymer.[14] This offers the potential for a better interface to be formed, leading to enhanced gas transport properties and other effects.

Super glassy polymers such as polyacetylenes demonstrate attractive initial permeability and selectivity properties, ease of processability and a capacity to be produced at industrial scale. However, as mentioned above, the industrial viability of this class of polymers is impaired by rapid physical aging processes.[1,15] For example, the CO_2 permeability of the super glassy polymer poly(1-trimethylsilyl-1)propyne (PTMSP) decreases to 27% of its as-cast value over one year (29 796 Barrer to 8045 Barrer) (Fig. 5(a) and (b)) as the large cavities collapse towards an unattainable thermodynamic equilibrium.[15]

Here, we explore a new form of molecular interaction within PTMSP-based mixed-matrix membranes. A systematic series of MOPs with varying extrinsic organic chain lengths were synthesized (Fig. 2). Each MOP is of the general form $[Cu_{24}(A)_{24}(S)_{24}]\cdot xS$, where A represents one of four aromatic di-acid ligands, S represents a solvent molecule. Each of the di-acids can be differentiated by their side chain chemistry and chain length: (a) non-polar *tert* butyl (^{t}Bu MOP; Fig. 2(c)); (b) polar diethylene glycol (DEG MOP; Fig. 2(d)); (c) polar triethylene glycol (TEG MOP; Fig. 2(e)) and non-polar dodecane (MOP-18; Fig. 2(f)). The ^{t}Bu MOP,[16] the DEG MOP[17] and MOP-18 [18] have been reported previously. The TEG MOP is a novel structure; differing from the DEG MOP, and the related tetraethylene glycol MOP[19] by one ethylene glycol group per di-acid ligand. Synthetic conditions and analytical data for the TEG MOP are available in the ESI.§

The nanoporous additives comprised of shorter side-groups were found to allow intercalation of polymer chains into the MOP pores, producing anti-aging intercalated membranes (AIMs) that exhibited superior anti-aging properties. The effect of polymer intercalation on the physical properties of the bulk of the polymer matrix was investigated using conventional analytical techniques. Of note, viscosity measurements provided a probing measure of additive–polymer interactions in solution form, and enabled additive loading optimization to

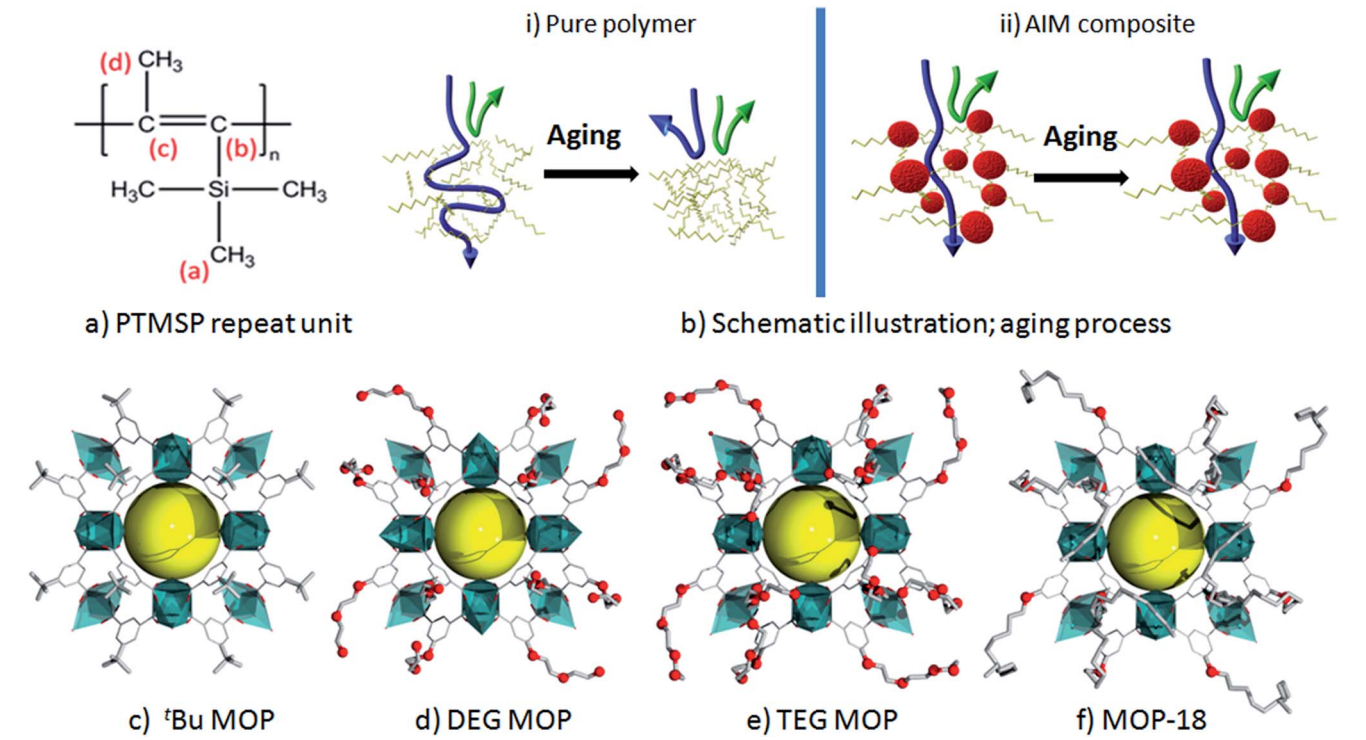

Fig. 2 (a) PTMSP repeat unit; (b) schematic illustrations of (i) pure polymer membrane exhibiting packing of polymer chains after aging, and (ii) MOP–MMM composite that prevents chain relaxation, maintaining membrane permeability; (c) ^{t}Bu MOP; (d) DEG-MOP; (e) TEG-MOP; and (f) MOP-18.

maximize anti-aging properties of the most successful AIM composition.

Experimental

MOP–PTMSP mixed-matrix membranes were produced through slow solvent evaporation following extensive pre-stirring of MOP–polymer solutions. Uniform distribution of MOP nanoparticles throughout the polymer matrix was confirmed using energy-dispersive X-ray spectroscopy (EDX) and focused ion beam scanning electron microscopy (FIB-SEM) (Fig. 4).

PTMSP was purchased from Gelest Inc. (Morrisville PA, USA) and used without purification. Chloroform was purchased from Sigma-Aldrich.

5 wt%, 10 wt%, 15 wt%, 20 wt%, 25 wt% and 30 wt% MOP + PTMSP membranes were fabricated through a typical spin casting method. The following is an example, for the 5 wt% loaded film.

200 mg PTMSP was placed in a 20 mL vial with 5 g chloroform and an egg-shaped stirrer bar and stirred overnight. A 10 mg ^{t}Bu MOP sample was placed in a separate 20 mL vial with 5 g chloroform and an egg-shaped stirrer bar. Each vial was closed and stirred for 24 hours under ambient conditions. Following this, the ^{t}Bu MOP–chloroform solution was added to the vial containing the stirred PTMSP–chloroform solution, and the mixed solution stirred for a further 24 hours under ambient conditions. ~100 micron films were formed *via* solution casting at ambient conditions. The membrane films were dried in a vacuum oven at 40 °C for 12 hours prior to single gas permeability measurements. Film thicknesses were measured using a Measumax digital micrometer.

Characterization methods

Scanning electron microscopy (SEM) was performed on a JEOL JEM 2100F TEM/SEM operated at 200 kV. EDS spectra were obtained using a JEOL 50 m^2 Si(Li) detector. FIB-SEM images were obtained at the Melbourne Centre for Nanofabrication. WAX experiments were performed on the SAX/WAX beamline at the Australian Synchrotron, Clayton, Victoria, Australia. Viscosity measurements were performed using an Ubbelohde viscometer at 25 °C, and calculated based on the ATSM D445 standard.

Results and discussion

One indicator of a beneficial polymer–particle interaction in a mixed-matrix membrane is the viscosity of a precursor solution. The viscosity of nanoparticle-filled polymer solutions drop in comparison to pure polymer melts where polymer chains can tether to the surface of the nanoporous additives and confine polymer chains within the mixed matrix.[20,21] Such an interaction involves an attraction between similar chemical groups of the polymer and additives that decreases the interchain entanglement of the bulk polymer solution.

To probe the extent of polymer–MOP interaction, viscosity tests were undertaken using an Ubbelohde Viscometer on pure PTMSP and additive–polymer blends stirred for 24 hours. This characterization technique has been used for several nanoparticle–membrane composites involving PAF-1, UiO-66 and fused silica as nanoporous additives.[9] These studies found that non-Newtonian behavior can arise in three situations: (1) where extra free volume is introduced;[20] (2) where polymer chains adsorb to the surface of the additive, decreasing polymer chain entanglement;[21] and (3) where polymer chains thread into the additives' pores.[21] In our previous work, we found that only in the case of the third interaction, that is, where polymer chains can thread into the additives' pores, is physical aging halted.[9,22]

The addition of MOPs with smaller chain lengths (^{t}Bu and DEG) led to an additive–polymer solution viscosity lower than that of pure PTMSP (11.725 cP and 12.244 cP compared to 12.733 cP) (Fig. 3(a)). The TEG + PTMSP blend was found to have a viscosity slightly above that of pure PTMSP (12.882 cP) In contrast, the MOP-18 + PTMSP blend was found to have a much higher viscosity (13.188 cP) than that of pure PTMSP (Fig. 3(a)).

The reduction in additive–polymer viscosity of solutions with smaller MOP side-chain lengths (^{t}Bu, DEG) indicates an interaction between additives and polymer chains. When compared with the anti-aging properties of the resulting films (Fig. 5(a) and (b)), we speculate that this decrease in viscosity results from

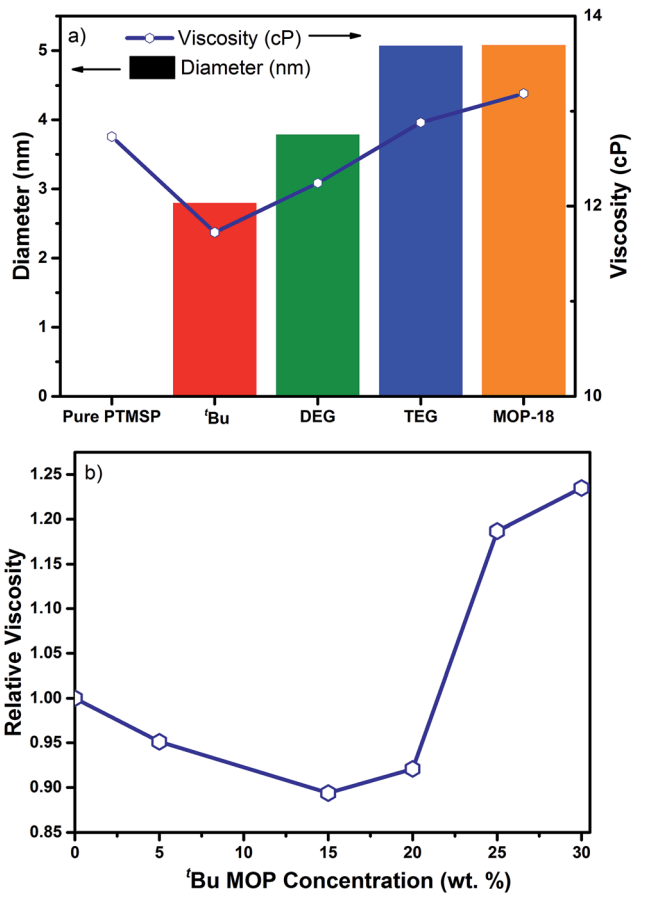

Fig. 3 (a) MOP–PTMSP solution viscosities (centiPoise) *vs.* MOP diameters; (b) ^{t}Bu MOP–PTMSP viscosities (centiPoise).

a decrease in inter-chain coupling of polymer chains through intercalation of polymer chains into the MOP pores. In contrast, the increase in viscosity of the 20 wt% MOP-18 + PTMSP blend, and the absence of anti-aging properties in the resulting membrane, suggests no interdigitation of polymer chains into the pores of the MOP.

The decrease in viscosity of the 20 wt% ^{t}Bu and DEG + PTMSP solutions can be explained through the concept of preferential tethering of polymer chains of higher molecular weight into the MOP pores, which leaves the lower molecular mass chains to constitute the bulk of the polymer matrix. This selective physisorption of high molar mass polymer fractions onto nanoporous additives is well documented.[23,24] Further, the resulting reduction in entanglement density of the lower molecular weight polymer bulk reduces viscosity through an increase in polymer flow.[25]

In this work, we also observed the concentration of nanoporous materials to have a significant effect on additive–polymer solution viscosities and resulting membrane properties. An increase in loading concentration of ^{t}Bu was found to decrease viscosities up to a minimum of 15 wt%. Above 20 wt%, loading, viscosity greatly increased (Fig. 3(b)).

Pore architecture effects of ^{t}Bu additives were studied with wide-angle X-ray scattering (WAXS) (Fig. 4(c)). Diffraction data of doped samples aged for 365 days was compared to that of pure PTMSP, and cross referenced with PTMSP WAX data found in literature.[26] The major peak at 9.8° corresponds to the small, channel-like cavities that have been found to be the transport pathway for gas molecules.[2] The smaller peaks at higher angles have been attributed to supramolecular ordering in PTMSP, arising from inter-chain spacing.[26] Importantly, the number of small holes decreases in the 5 wt% and 30 wt% samples over time, as indicated by the lower area under these peaks, and as represented by reduced gas permeabilities in these aged samples. Conversely, for the 20 wt% doped sample a large number of pores was maintained over time, as represented by the large area under the lower-angle peak.

The single gas permeabilities and ideal selectivities of MOP-loaded films taken of freshly-cast polymers and again after one year of exposure to the atmosphere can be seen in Fig. 5(a) and S3–S7.§ The corresponding data for a film of pure PTMSP treated under the same conditions is also provided for comparison.

The initial CO_2 permeabilities of 20 wt% loaded ^{t}Bu + PTMSP, DEG + PTMSP and TEG + PTMSP films are comparable, each being approximately 5000 Barrer lower than that of pure PTMSP (Fig. 5(a)). Altering MOP loadings of the ^{t}Bu series also had a negligible effect on initial permeabilities (Fig. 5(b)). This suggests that permeation is controlled by the polymer rather than the MOP additives, with pores of each MOP being inaccessible to these gases over the pressure range studied. On the contrary, the initial permeability of 20 wt% MOP-18 + PTMSP is much lower than that of pure PTMSP (Fig. 5(a)). This is attributed to the presence of the long dodecane chains of the MOP-18

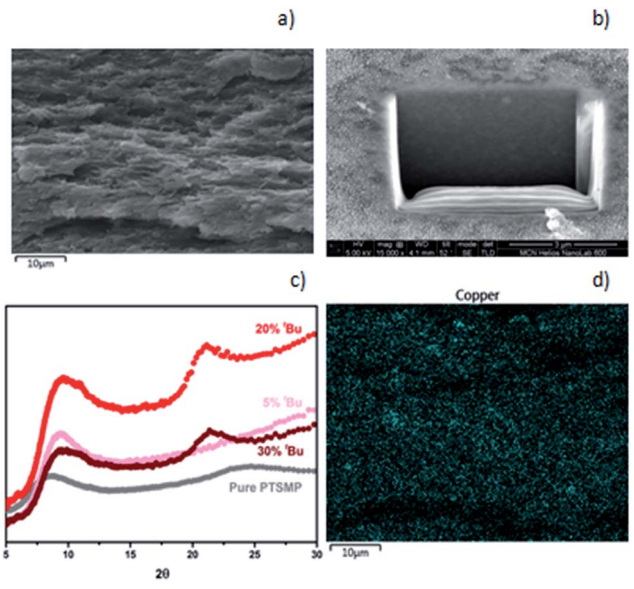

Fig. 4 (a) FIB-SEM of a milled 20 wt%-doped ^{t}Bu PTMSP membrane showing uniform dispersion of MOP nanoparticles (b) EDX data of a 20 wt% ^{t}Bu loaded PTMSP membrane, (c) WAX data of ^{t}Bu PTMSP samples. (d) EDS spectra of the cross section of a 20 wt% ^{t}Bu + PTMSP film showing even dispersion of MOP particles throughout the film.

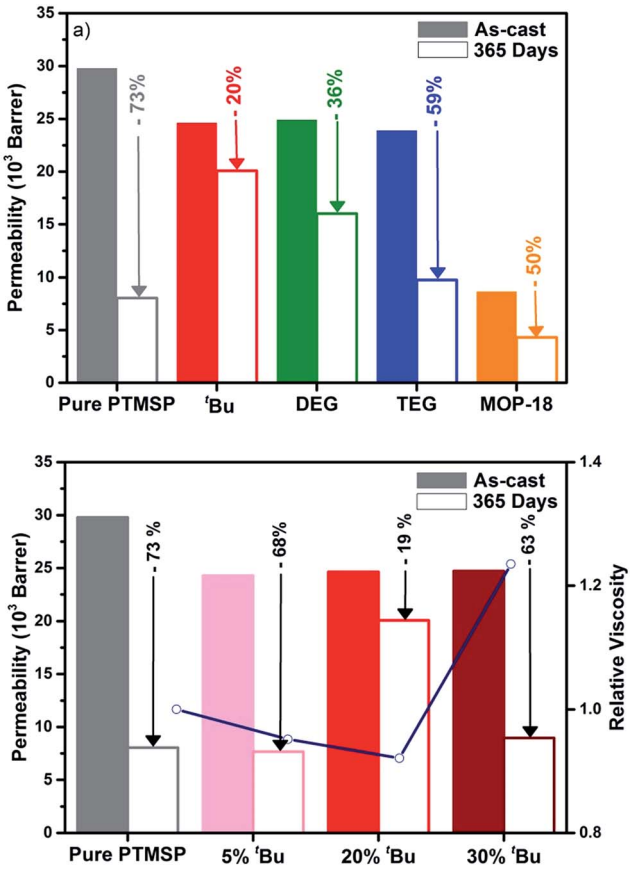

Fig. 5 (a) CO_2 permeability properties of 20 wt% MOP-loaded PTMSP membranes as cast *vs.* 365 days; (b) CO_2 permeability properties of ^{t}Bu–PTMSP membranes of different dopant loadings as cast *vs.* 365 days.

side groups, which block polymer pores, obstructing gas pathways.[14]

Addition of 20 wt% ^{t}Bu, DEG and TEG MOPs stopped the aging of PTMSP, to different degrees. Of the AIMs investigated, the 20 wt% loading of ^{t}Bu was most successful at freezing the super-glassy polymer in its initial state, with CO_2 permeability reducing to only 81% of its as-cast value over one year (Fig. 5(a)). This represents a 250% improvement when compared with the CO_2 permeability of a pure PTMSP film after one year (27% of its as-cast value). The DEG + PTMSP film, loaded with the shorter ethylene glycol-based MOP, had a greater anti-aging effect than the longer TEG + PTMSP film, with the CO_2 permeability of each reducing to 64% and 41% respectively (Fig. 5(a)). The CO_2 permeability of the MOP-18 + PTMSP film decreased to 50% of its as-cast value, which, given the low as-cast properties of the film, represents a permeability lower than that of pure PTMSP (Fig. 5(a)).

With the exception of MOP-18 + PTMSP, the selectivity of the MOP + PTMSP films changed proportionately over the space of a year, increasing as permeability decreased (Fig. S3–S7§). The change in CO_2/CH_4 selectivity of MOP-18 + PTMSP deviated from that of both the MOP-loaded films and the pure PTMSP film, showing a higher relative selectivity for CH_4 than that of the other films investigated, and therefore a decrease in selectivity despite the lower permeability of the aged film. This suggests that the CH_4 molecules compete for the sorption sites associated with MOP-18 alkyl chains in the polymer blend.[14]

Notably, the different chemical nature of the non-polar saturated hydrocarbons and the polar polyethylene glycol side chains did not dominate the aging properties of the MOP-loaded films. These results suggest that PTMSP–MOP pore intercalation is dominated by the length, rather than chemistry, of the additive side chain.

The kinetics of physical aging in a polymer is closely related to the molecular mobility of the polymer chains in the glassy state.[27,28] The preferential tethering of high molecular weight polymer chains into the pores of the ^{t}Bu, DEG and TEG + PTMSP solutions can therefore be regarded as complementing the observed anti-aging properties of their corresponding films. Confinement of these larger chains leaves those chains of lower molecular weight to make up the bulk of the polymer matrix. Polymer chains of lower molecular weight exhibit less flexibility than that of longer polymer chains, and as a result do not have the conformational freedom to relax into a more dense packing state. As observed from the permeability of aged ^{t}Bu + PTMSP, DEG + PTMSP and TEG + PTMSP films, this confinement of higher molecular mass polymer chains leads to a decrease in physical aging, resulting in less dense polymer films over time when compared to the 20 wt% MOP-18 + PTMSP and pure PTMSP films.

The concept of optimal loading fractions in polymer melts has been reported for several decades, and can be explained through a study of polymer interactions and interparticle distances.[20,29] Whereas intercalated polymer chains are rigidified, free polymer chains retain conformational flexibility, which drives physical aging. At additive concentrations below the percolation threshold, the relative number of intercalated polymer chains is low, and a large amount of the polymer bulk consists of free, large polymer chains. A reduction in chain entanglement of the resulting bulk solution results in a decrease in viscosity relative to pure PTMSP, as observed in Fig. 2(a). The reduction in chain entanglement of the bulk solution also loosens steric hindrances on the rotational motions of these free polymer chain side groups. This allows for greater chain flexibility, and therefore aging of the low-loaded films, as observed in Fig. 5(b).[30]

At an optimal loading concentration, all large polymer chains are intercalated. The lower viscosity of the solution can therefore be explained in terms of a further decrease in chain entanglements (Fig. 2(b)). The absence of free polymer chains also explains the suppression of physical aging in the 20 wt% loaded film, as polymer flexibility is restrained (Fig. 5(a) and (b)).

Above this optimal loading concentration, the MOP interparticle distances are reduced, leading to entanglement of intercalated chains. This results in a large increase in the viscosity, as observed in the 30 wt% loaded solution (Fig. 2(b)). Further, MOP interparticle distances are greatly reduced, and given the insufficient polymer chains present to fully interact with the MOP particles, multiple interactions with adjacent nanoparticles is possible.[31] The entanglement of intercalated chains into neighbouring MOPs allows aggregation of the additives, resulting in a reduction of polymer free volume and decreasing membrane permeability (Fig. 5(b)).

Mathematical modeling was used to further substantiate our results. Effective size calculations were carried out, which consider the van der Waals radii of each atom, as defined according to Bondi.[32] The trimethylsilyl (TMS) side group of PTMSP has an effective size of 6.3 Å. The effective size of the outer cavity of the ^{t}Bu MOP is 10 Å, suggesting that the trimethylsilyl side groups of the PTMSP polymer can intercalate into ^{t}Bu MOP pores, forming an interlocked configuration (Fig. 6).

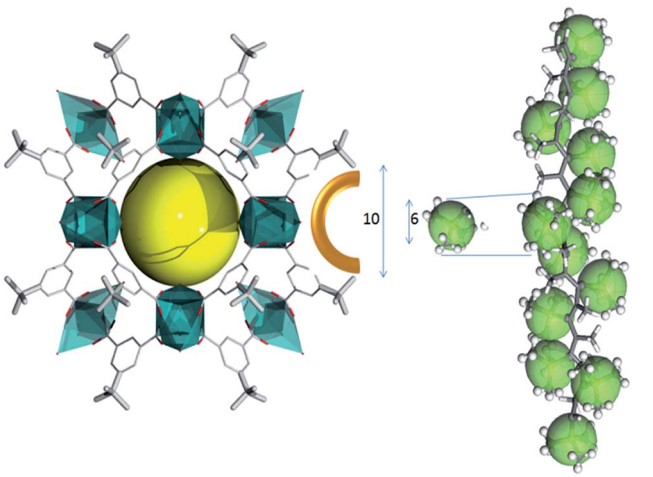

Fig. 6 The largest ^{t}Bu MOP pore windows are large enough (13.671 Å) to allow intercalation of PTMSP trimethylsilyl groups into the MOP pore.

Conclusions

Introducing MOP nanoparticles as inorganic additives, we synthesized a series of related AIMs. Varying the length and chemistry of nanoparticle side-groups allowed us probe the polymer–additive interfacial conditions required to allow for beneficial, non-covalent molecular interlocking of polymer chains. The effect of polymer intercalation on the physical properties of the bulk of the polymer matrix was also investigated.

Superior dispersion of MOP nanoparticles throughout PTMSP was observed using EDX and FIB-SEM. The large surface area to volume ratios of MOP nanoparticles was found to allow for increased interaction between polymer chains and nanoparticle pores. Viscosity results suggest a correlation between additive side-chain length and polymer chain interaction, with smaller side-chains of the ^{t}Bu nanoparticles allowing greater intercalation of the polymer chains into the MOP pores. No trend in polymer–additive interfacial properties was observed in relation to nanoparticle side-group chemistry. Comparing viscosity results with permeabilities of fresh and aged samples, it appears that the greater this intercalation, the more fractional free volume that is retained over time. Through comparison of different MOP loading concentrations, it was found that a decrease in interchain entanglement of polymer solutions resulting from preferential tethering of higher molecular weight polymer chains leads to a reduction in polymer aging, as smaller, less flexible chains remaining in the polymer bulk lack in conformational freedom required to relax into a more dense packing state.

Abbreviations

MOP	Metal-organic polyhedra
MMM	Mixed-matrix membrane
PTMSP	Poly(1-trimethylsilyl-1-propyne)

Acknowledgements

Parts of this work were conducted on the SAXS Beamline at the Australian Synchrotron and the Melbourne Centre for Nanofabrication. The authors acknowledge Dr Cameron Way for assistance with viscosity measurements.

Notes and references

1 H. B. Park, C. H. Jung, Y. M. Lee, A. J. Jill, S. J. Pas, S. T. Mudie, E. V. Wagner, B. D. Freeman and D. J. Cookson, *Science*, 2007, **318**, 254–258.
2 K. Nagai, T. Masuda, T. Nakagawa, B. D. Freeman and I. Pinnau, *Prog. Polym. Sci.*, 2001, **26**, 721–798.
3 S. Fu, E. S. Sanders, S. S. Kulkarni and W. J. Koros, *J. Membr. Sci.*, 2015, **487**, 60–73.
4 D. M. D'Alessandro, B. Smit and J. R. Long, *Angew. Chem., Int. Ed.*, 2010, **49**, 6058–6082.
5 T. C. Merkel, L. G. Toy, A. L. Andrady, H. Gracz and E. O. Stejksal, *Macromolecules*, 2003, **36**, 353–358.
6 Y. C. Hudiono, T. K. Carlisle, J. E. Bara, Y. Zhang, D. L. Gin and R. D. Noble, *J. Membr. Sci.*, 2010, **350**, 117–123.
7 T. C. Merkel, B. D. Freeman, R. J. Spontak, Z. He, I. Pinnau, P. Meakin and A. J. Hill, *Science*, 2002, **19**, 519–522.
8 G. Dong, H. Li and V. Chen, *J. Mater. Chem. A*, 2013, **1**, 4610–4630.
9 (*a*) C. H. Lau, P. T. Nguyen, M. R. Hill, A. W. Thornton, K. Konstas, C. M. Doherty, R. J. Mulder, L. Bourgeois, A. C. Y. Yiu, D. J. Sprouster, J. P. Sullivan, T. J. Bastow, A. J. Hill, D. L. Gin and R. D. Noble, *Angew. Chem., Int. Ed.*, 2014, **53**, 5322–5326; (*b*) C. H. Lau, K. Konstas, C. M. Doherty, S. Kanehashi, B. Ozcelik, S. E. Kentish, A. J. Hill and M. R. Hill, *Chem. Mat.*, 2015, DOI: 10.1021/acs.chemmater.5b01537.
10 S. Shu, S. Husain and W. J. Koros, *J. Phys. Chem. C*, 2007, **111**, 652–657.
11 J. S. Wall, B. Hu, J. A. Siddiqui and R. M. Ottenbrite, *Langmuir*, 2001, **17**, 6027–6029.
12 T. Ben, H. Ren, S. Ma, D. C. Prof, J. Lan, X. Jing, W. Wang, J. Xu, F. Deng, J. M. Simmons, S. Qiu and G. Zhu, *Angew. Chem., Int. Ed.*, 2009, **48**, 9457–9460.
13 M. Eddaoudi, J. Kim, J. B. Wachter, H. K. Chae, M. O'Keeffe and O. M. Yaghi, *J. Am. Chem. Soc.*, 2001, **123**, 4368–4369.
14 E. V. Perez, K. J. Balkus, J. P. Ferraris and I. H. Musselman, *J. Membr. Sci.*, 2014, **463**, 82–93.
15 K. Nagai, T. Masuda, T. Nakagawa, B. D. Freeman and I. Pinnau, *Prog. Polym. Sci.*, 2001, **26**, 721–798.
16 J.-R. Li and H.-C. Zhou, *Nat. Chem.*, 2010, **2**, 893–898.
17 M. Tonigold and D. Volkmer, *Inorg. Chim. Acta*, 2010, **363**, 4220–4229.
18 H. Furukawa, J. Kim, K. E. Plass and O. M. Yaghi, *J. Am. Chem. Soc.*, 2006, **128**, 8398–8399.
19 M. S. Tonigold, *Novel Copper- and Cobalt-based Metal-Organic Polyhedra and Frameworks: Synthesis, Structure, Properties and Applications*, Ulm University, 2011.
20 M. E. Mackay, T. T. Dao, A. Tuteja, D. L. Ho, B. V. Horn, H.-C. Kim and C. J. Hawker, *Nat. Mater.*, 2003, **2**, 762–766.
21 S. Jain, J. G. P. Goossens, G. W. M. Peters, M. V. Duin and P. J. Lemstra, *Soft Matter*, 2008, **4**, 1848–1854.
22 C. H. Lau, K. Konstas, A. W. Thornton, A. C. Liu, S. Mudie, D. F. Kennedy, S. C. Howard, A. J. Hill and M. R. Hill, *Angew. Chem., Int. Ed.*, 2015, **54**, 2669–2673.
23 F. H. J. Maurer, H. M. Schoffeleer, R. Kosfeld and T. Uhlenbroich, *Progress in Science and Engineering of Composites*, ICCM-Iv, Tokyo, 1982.
24 R. E. Felter, E. S. Moyer and Z. N. Ray, *J. Polym. Sci., Part B: Polym. Lett.*, 1969, **7**, 529–533.
25 O. Kramer, V. Ty and J. D. Ferry, *Proc. Natl. Acad. Sci. U. S. A.*, 1972, **69**, 2216–2218.
26 Y. U. P. Yampol'skii, S. M. Shishatskii, V. P. Shantorovich, E. M. Antipov, N. N. Kuzmin, S. V. Rykov, V. L. Khodjaeva and N. A. Plate, *J. Appl. Polym. Sci.*, 1993, **48**, 1935–1944.
27 A. J. Kovacs, J. J. Aklonis, J. M. Hutchinson and A. R. Ramos, *J. Polym. Sci., Polym. Phys. Ed.*, 2003, **17**, 1097–1162.

28 V. M. Boucher, D. Cangialosi, A. Alegria, J. Colmenero, J. Gonzalez-Irun and L. M. Liz-Marzan, *Soft Matter*, 2010, **6**, 3306–3317.
29 R. K. Iler, *J. Colloid Interface Sci.*, 1971, **37**, 364–373.
30 I. M. Kalogeras and A. Vassilikou-Dova, *J. Phys. Chem. B*, 2001, **105**, 7651–7662.
31 T. Cosgrove, P. C. Griffiths and P. M. Lloyd, *Langmuir*, 1995, **11**, 1457–1463.
32 A. Bondi, *J. Phys. Chem.*, 1964, **68**, 441–451.